

# Quantum Dot/Siloxane Composite Film Exceptionally Stable against Oxidation under Heat and Moisture

Hwea Yoon Kim,<sup>†</sup> Da-Eun Yoon,<sup>‡</sup> Junho Jang,<sup>†</sup> Daewon Lee,<sup>†</sup> Gwang-Mun Choi,<sup>†</sup> Joon Ha Chang,<sup>§</sup> Jeong Yong Lee,<sup>§</sup> Doh C. Lee,<sup>\*,‡</sup> and Byeong-Soo Bae<sup>\*,†</sup>

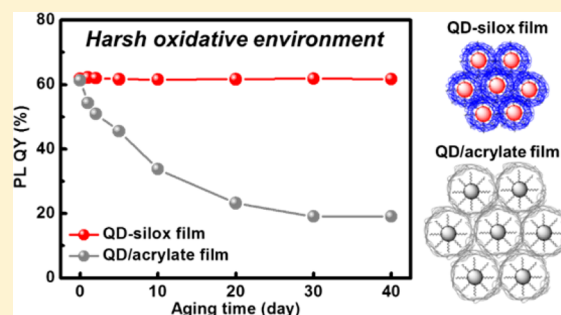
<sup>†</sup>Department of Materials Science and Engineering, KAIST Institute for the Nanocentury, Korea Advanced Institute of Science and Technology (KAIST), Daejeon 34141, Korea

<sup>‡</sup>Department of Chemical and Biomolecular Engineering, KAIST Institute for the Nanocentury, Daejeon 34141, Korea

<sup>§</sup>Center for Nanomaterials and Chemical Reactions, Institute for Basic Science (IBS), Daejeon 34141, Korea

## Supporting Information

**ABSTRACT:** We report on the fabrication of a siloxane-encapsulated quantum dot (QD) film (QD-silox film), which exhibits stable emission intensity for over 1 month even at elevated temperature and humidity. QD-silox films are solidified via free radical addition reaction between oligosiloxane resin and ligand molecules on QDs. We prepare the QD-oligosiloxane resin by sol-gel condensation reaction of silane precursors with QDs blended in the precursor solution, forgoing ligand-exchange of QDs. The resulting QD-oligosiloxane resin remains optically clear after 40 days of storage, in contrast to other QD-containing resins which turn turbid and ultimately form sediments. QDs also disperse uniformly in the QD-silox film, whose photoluminescence (PL) quantum yield (QY) remains nearly unaltered under harsh conditions; for example, 85 °C/5% relative humidity (RH), 85 °C/85% RH, strongly acidic, and strongly basic environments for 40 days. The QD-silox film appears to remain equally emissive even after being immersed into boiling water (100 °C). Interestingly, the PL QY of the QD-silox film noticeably increases when the film is exposed to a moist environment, which opens a new, facile avenue to curing dimmed QD-containing films. Given its excellent stability, we envision that the QD-silox film is best suited in display applications, particularly as a PL-type down-conversion layer.



## INTRODUCTION

Semiconductor nanocrystals in the quantum confinement regime, also known as quantum dots (QDs), have attracted a tremendous amount of interest, particularly since the arrested precipitation approach allowed for scalable chemical synthesis of high-quality colloidal QDs.<sup>1,2</sup> Central to the colloidal synthesis of QDs is the use of organic ligands that keep the resulting QDs uniform in size, soluble in various organic solvents, and highly luminescent with photoluminescence (PL) quantum yield (QY) relatively stable over time as surface dangling bonds are passivated.<sup>3–6</sup> In attempts to capitalize on the unique optical properties of QDs, such as tunable energy gap and narrow emission bandwidth, QD/polymer composites, in which QDs are physically blended in polymer matrices, have been prepared and used within the context of down-conversion of light from solid-state light-emitting diodes (LEDs) for display applications.<sup>7–9</sup>

Despite significant research efforts, the fabrication of commercially viable QD/polymer composites face a couple of formidable roadblocks: (i) poor dispersion of QDs in polymer; and (ii) deteriorating optical properties, such as PL QY, of the composites. Simple mixing results in aggregation and/or phase separation of QDs from polymer matrices.<sup>10–12</sup> One way of

solving this problem is to replace organic ligands on the surface of QDs via ligand exchange into molecules, e.g., thiols, phosphines and amines, with functionalities that enable the QDs to disperse better in such polymer composites.<sup>13–15</sup> However, the PL QY of the QDs inevitably decreases during the ligand-exchange procedures.<sup>16–18</sup> In addition to the dispersion problem, the PL QY of the QD/polymer composite film decreases over time, particularly when the film is exposed to heat, oxygen, or moisture.<sup>19,20</sup> In fact, commercially available QD/polymer films currently adopted in display applications use barrier layers to keep the composites from oxygen and moisture, and the additional layers make the films economically less competitive.<sup>21</sup> The ultimate quest to barrier-film-free composites demands an ultrastable QD/polymer film to keep their optical properties even under exposure to air and moisture.

Sol-gel condensation reaction of silane precursors to synthesize siloxane-containing film has been intensively studied and utilized in the past few decades, as the resulting films help encapsulated molecules, such as enzymes, catalysts, and

Received: October 12, 2016

Published: November 29, 2016

fluorescent dyes, retain their intrinsic properties.<sup>22–24</sup> The hallmark of the siloxane-based matrix is its high thermal stability compared to hydrocarbon-based polymers, because of the silica (SiO<sub>2</sub>)-like amorphous networks by Si—O—Si bonds.<sup>25</sup> Recently, we reported a dye-siloxane composite film which shows long-term stability at high temperatures.<sup>24</sup> The encapsulation of dyes by heat resistive siloxane matrix accounts for the long-term stable fluorescence of dye-siloxane film.

Here, we investigate stability of siloxane-encapsulated QD composite film by preparing CdSe/ZnS core/shell QDs embedded in siloxane film (denoted hereafter as QD-silox film). The composite is fabricated via UV-induced free radical addition reaction of oligosiloxane resin in which the QDs are blended (denoted hereafter as QD-oligosiloxane resin). 3-Methacryloxypropyltrimethoxysilane (MPTS) and diphenylsilanediol (DPSD) were used as silane precursors to form viscous oligosiloxane resin via sol-gel condensation reaction in the presence of CdSe/ZnS core/shell QDs passivated by oleic acid (OA). We analyzed the dispersibility of the QD-oligosiloxane resin in the context of examining the dispersibility and colloidal stability of QDs within oligosiloxane matrix. To compare properties of QD-oligosiloxane resin and QD-silox film, diacrylate functionalized aliphatic oligomer resin was selected as a reference matrix because it contains acryl functional groups and no siloxane bonds. The comparison provides some perspective on the stability of QD-silox film, as the acrylate polymer has been widely used to prepare QD/polymer composite films.

## RESULTS AND DISCUSSION

We prepared the QD-silox film via UV-induced cross-linking of free radical addition reaction to solidify the CdSe/ZnS QDs in oligosiloxane resin (concentration of QDs: 0.5 wt %) which was synthesized by sol-gel condensation reaction between silane precursors of 3-methacryloxypropyltrimethoxysilane (MPTS) and diphenylsilanediol (DPSD). Optical properties of the QD-silox film were analyzed in reference to the QD/acrylate film, which was prepared by blending the same batch of CdSe/ZnS QDs in acrylate oligomer resin (molecular weight: 468) for 4 h at 80 °C under N<sub>2</sub>, and solidifying the blend by UV-induced cross-linking. Figure 1A shows traces of PL QY of QD-silox and QD/acrylate films monitored for 40 days of aging in air at 85 °C and 5% relative humidity (RH) for 40 days. The QD-silox film maintains the initial PL QY, while the QD/acrylate film exhibits drastic decrease of PL QY from 61.3% to 19.6%, during aging for 40 days.

We also measured PL decay dynamics to characterize the optical properties of QD-silox and QD/acrylate films before and after aging in air at 85 °C (Figure 1B). We define the PL lifetime ( $\tau$ ) to be the time at which PL intensity from the sample is 1/e times the initial intensity (i.e., 1/e lifetime). The QD-silox film maintains the initial PL lifetime, whereas the QD/acrylate film exhibits severe diminish of PL lifetime from 35.3 to 4.6 ns, during aging for 40 days, alluding to the oxidation of QDs in the QD/acrylate film during the aging. Fitting of PL decay traces to either single-exponential or multiexponential curve is carried out to establish a proposition on the nonradiative and radiative recombination decay pathways. The PL intensity decay dynamics of QD-silox and QD/acrylate films before the accelerated aging are fitted with biexponential decay with two recombination components;  $\tau_1$ : 34.4 ns (98.4%) and  $\tau_d$ : 192.2 ns (1.3%), where percentage in parentheses denotes population of the component. The faster

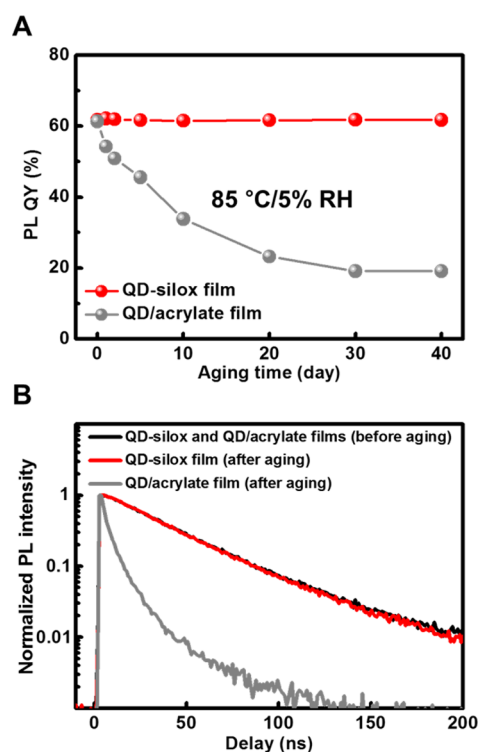


**Figure 1.** (A) Traces of PL QY of QD-silox film (red) and QD/acrylate film (gray) monitored over 40 days of aging in air at 85 °C and 5% relative humidity (RH). (B) PL decay dynamics of QD-silox and QD/acrylate films before (black) and after (red: QD-silox; and gray: QD/acrylate) aging for 40 days.

decay component (20–40 ns) is assigned to radiative recombination, and the slower to delayed recombination pathway beyond time scale of 100 ns.<sup>26</sup> The delayed recombination lifetime indicates the existence of long-lived trap states developed in the surrounding of QDs; in our case, siloxane or acrylate matrix.<sup>26</sup> Biexponential fitting of the PL decay curve for the aged QD-silox film yields similar values of radiative ( $\tau_1$ : 33.4 ns, 98.1%) and delayed recombination lifetimes ( $\tau_d$ : 157.2 ns, 1.9%). However, the PL decay curve from the aged QD/acrylate film does not show the delayed recombination component. The fitting gives rise to new fast, nonradiative ( $\tau_1$ : 4.6 ns, 88.8%) and slow, radiative recombination components ( $\tau_2$ : 23.5 ns, 11.1%). The new fast decay component and reduced population of radiative recombination pathways point to possibility that trap states are formed after aging the QD/acrylate film in air at 85 °C. We speculate that formation of new trap states promotes nonradiative recombination and effectively suppresses radiative recombination. Therefore, formation of the new nonradiative recombination channel is responsible for decreased PL QY of the aged QD/acrylate film. Conversely, unchanged PL decay dynamics in the case of the QD-silox film after aging is in accordance with the relatively unaltered PL QY after the aging step. We ascribe the long-term stability of PL QY in the case of QD-silox film to uniform passivation of QDs by oligosiloxane matrix which may act as an amorphous SiO<sub>2</sub>-like passivation layer around the QDs.<sup>23,25</sup>

To unveil the molecular origin of the enhanced PL QY stability of our QD-silox film, the fabrication process of QD-silox film needs to be dissected. Our QD-silox film is fabricated via three steps (Figure 2). First, CdSe/ZnS QDs are dispersed

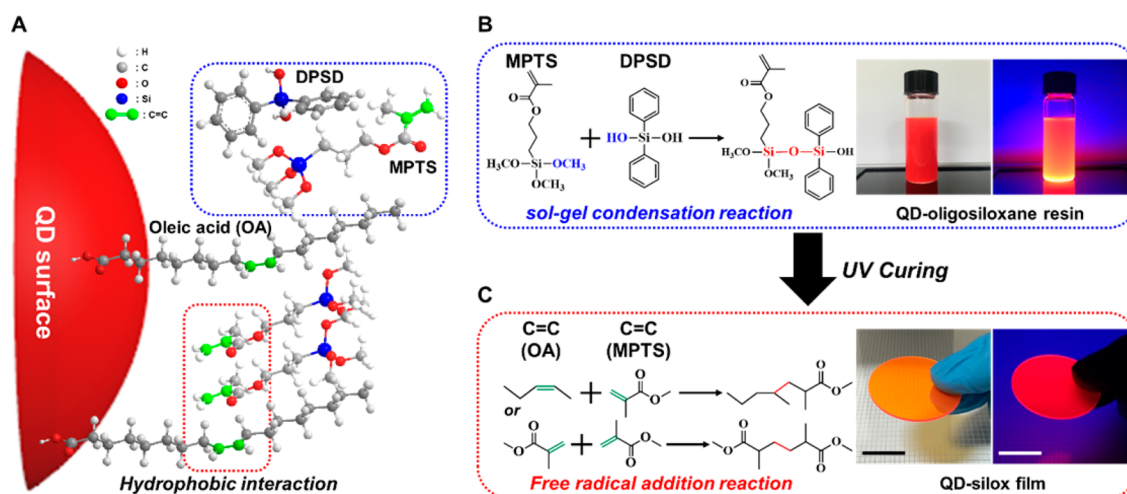


**Figure 2.** Schematic illustration of fabrication process of QD-silox film. (A) Hydrophobic interaction between silane precursors (MPTS and DPSD) and ligands (oleic acid) on QDs. (B) Sol-gel condensation reaction between MPTS and DPSD. Inset shows photographs of QD-oligosiloxane resin under room light (left) and UV lamp ( $\lambda = 365 \text{ nm}$ ) (right). (C) Free radical addition reactions among carbon double bonds of methacryl functional groups and oleic acids. Inset shows photographs of QD-silox film under room light (left) and UV lamp ( $\lambda = 365 \text{ nm}$ ) (right). Scale bars are 20 mm.

in the mixture of silane precursors, which are composed of MPTS and DPSD (Figure 2A). During this step, hydrophobic interaction between oleic acid (surface ligand on QDs) and methacryl and phenyl functional groups of the silane precursors triggers encapsulation of the QDs by sol-gel condensation reaction.<sup>27,28</sup> In the second step, the siloxane bonds of the siloxane network are formed by sol-gel condensation reaction between methoxy groups of MPTS and hydroxyl groups of DPSD at the vicinity of QDs, resulting in homogeneous QD/oligosiloxane mixture (Figure 2B).<sup>29</sup> The resulting viscous QD-oligosiloxane resin shows no hint of flocculation, and PL QY remains nearly the same (the inset images of Figure 2B and Table S1 of the Supporting Information). Finally, a QD-silox film was fabricated by irradiating UV light onto the QD-oligosiloxane resin (see the inset images of Figure 2C).<sup>30</sup> As shown in Figure 2C, this free radical addition reaction of the QD-oligosiloxane resin results in the formation of carbon single bonds in two cross-linking reaction pathways: (i) the reaction between C=C bonds of methacryl functional groups of oligosiloxane matrix; and (ii) the reaction between C=C bonds of the methacryl functional group and oleic acid.<sup>31</sup> Either one of these two cross-linking pathways is responsible for rigid encapsulation of QDs by sol-gel-derived siloxane matrix.

After a free radical addition reaction that results in cross-linking of acrylic bonds, the PL QY of the QD-silox film (61.8%) becomes lower than that of QD-oligosiloxane resin (64.7%) (Figure S1). This slight decrease is attributed to higher contents of methacryl functional groups in QD-oligosiloxane resin, which leads to volumetric shrinkage upon the free radical addition reaction.<sup>32</sup> Such volumetric shrinkage of the QD-oligosiloxane resin effectively raises the volumetric concentration of QDs and the reabsorption of emitted photons by neighboring QDs increases, causing the PL QY to decrease after the cross-linking.<sup>33</sup> Likewise, PL QY of both QD-oligosiloxane resin and QD-silox film are decreased as the concentration of QDs increases, due to reabsorption of photons by QDs in vicinity (Figure S1).

Formation of siloxane bonds via sol-gel condensation reaction is confirmed by the <sup>29</sup>Si nuclear magnetic resonance (<sup>29</sup>Si NMR) analysis on QD-oligosiloxane resin (Figure 3A). As shown in the chemical formula in inset of Figure 3A, the

monomeric, dimeric, and trimeric species of Si atoms in siloxane bonds exist in the QD-oligosiloxane resin, and are represented by the terms of D<sup>n</sup> and T<sup>n</sup>, with the superscript “n” denoting the number of siloxane bonds of the Si atoms. The <sup>29</sup>Si NMR spectrum of the QD-oligosiloxane resin shows successful formation of siloxane network which is confirmed by both the absence of precursor species, DPSD (D<sup>0</sup>) and MPTS (T<sup>0</sup>) and detection of mono- (D<sup>1</sup> and T<sup>1</sup>), di- (D<sup>2</sup> and T<sup>2</sup>), and trimeric (T<sup>3</sup>) species. The degree of siloxane bond condensation (DOC) is calculated by the peak area of <sup>29</sup>Si NMR spectrum (Table S2). The calculated DOC value is 86.2%, which indicates the successful formation of an SiO<sub>2</sub>-like amorphous siloxane network present in QD-oligosiloxane resin.

Figure 3B shows Fourier-transform infrared (FT-IR) spectra of a QD-oligosiloxane resin and a QD-silox film. Bands corresponding to the stretching of siloxane bond (Si—O—Si) at 1100–1000 cm<sup>-1</sup> are present in both QD-oligosiloxane resin and QD-silox film, which supports the formation of siloxane network from the <sup>29</sup>Si NMR analysis on QD-oligosiloxane resin. Moreover, bands corresponding to the carbon double bond (C=C) at 1680–1630 cm<sup>-1</sup> (stretching) and 1000–950 cm<sup>-1</sup> (=CH out-of-plane deformation) of QD-oligosiloxane resin are likely detected from methacryl group in oligosiloxane matrix and oleic acid on QD surface. Disappearance of the bands corresponding to C=C in the QD-silox film manifests that the cross-linking occurs by free radical addition reaction among carbon double bonds in methacryl group and oleic acid in QD-oligosiloxane resin. Note that the high degree of siloxane bond formation and cross-linked bondings are the core mechanism for the rigid encapsulation of the QDs by siloxane matrix.<sup>22–24</sup>

Another testament to efficient passivation by cross-linked acrylic bonds between ligand of QDs and siloxane matrix is also available from thermogravimetric analysis (TGA) on bare siloxane film without QDs and QD-silox film. As shown in Figure 3C, the QD-silox film shows the higher thermal stability compared to bare siloxane film: the temperatures at which 1% weight loss occurs ( $T_{d1\%}$ ) are 300 and 275 °C for the QD-silox film and the bare siloxane film, respectively. The formation of additional acrylic bonds that cross-linked between ligands on the QDs and siloxane matrix leads to improved thermal stability

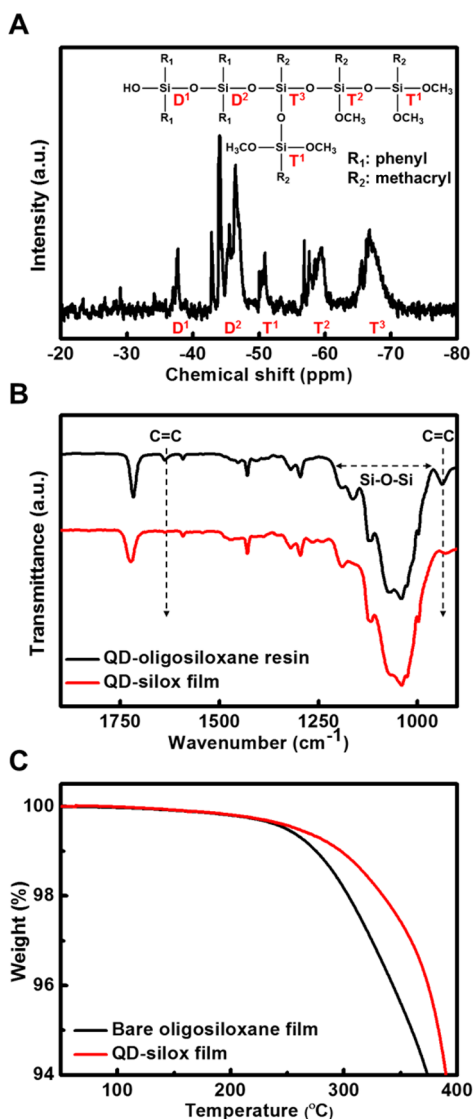


**Figure 3.** (A)  $^{29}\text{Si}$  NMR spectrum of QD-oligosiloxane resin. (Inset) Chemical structure of the QD-oligosiloxane resin representing Si atoms with different bond states. (B) FT-IR spectra of QD-oligosiloxane resin (black) and QD-silox film (red). (C) TGA profiles of bare siloxane film without QDs (black) and QD-silox film (red) (Ramping rate:  $10\text{ }^\circ\text{C}/\text{min}$ , under  $\text{N}_2$ ).

of the QD-silox film, while additional acrylic bonds are not formed in bare siloxane film. Furthermore, thermal degradation of QD-silox film occurs at higher temperature than the case of QD/acrylate film, which exhibits  $T_{d10\%}$  of  $230\text{ }^\circ\text{C}$  (Figure S2). In terms of chemical structure, the QD-silox film is mostly composed of Si—O bonds whose bonding energy is  $452\text{ kJ/mol}$ , while the QD/acrylate film contains majority part of carbon single bonds whose bonding energy is  $346\text{ kJ/mol}$ . This structural difference underlies the long-term PL QY stability of our QD-silox film under highly oxidative environment.

In the context of using the QD/polymer composite film in display devices, dispersion of QDs in the film will be a critical requirement, as uneven distribution could result in scattering of the light and blurred image from final products. We tested the uniformity of QD dispersion in the QD-oligosiloxane resin and QD-silox film using UV/vis spectroscopy, PL spectroscopy, dispersion stability analyzer, transmission electron microscopy (TEM), and time-of-flight secondary ion mass spectroscopy

(TOF-SIMS) (Figure 4). As shown in Figure 4A, the absorbance and PL spectra of QD-chloroform solution, QD-oligosiloxane resin, and QD-silox film reveal the uniform dispersion of QDs: the 1S peak wavelength, emission peak wavelength, and full width at half-maximum (fwhm) remain unchanged along the film fabrication processes (Table S3).

More direct observation of long-term dispersion stability of QD-oligosiloxane resin is enabled by Turbiscan, which records changes of light transmission. Over 40 days of storage, the QD-oligosiloxane resin exhibits little to no change of transmission, indicating that uniform dispersion of QDs within the resin mixture is maintained (Figure 4B). This good dispersion stability of QD-oligosiloxane resin can be ascribed to hydrophobic interaction between high content of hydrophobic functional groups (methacryl and phenyl) of oligosiloxane matrix and ligands (oleic acid) on QDs.<sup>27,28</sup> On the contrary, QD/acrylate resin shows noticeable aggregation within 1 h after QDs are blended with acrylate oligomer resin, because of relatively low wettability of acrylate oligomer matrix onto the oleate-rich QD surface (inset of Figure 4B).

In addition to previous optical analysis, structural analysis on QD-silox film was also conducted to confirm the even dispersion of QDs. For TEM analysis of QD-silox film, the sample was prepared by focused ion beam instrument (FIB). As shown in the TEM image of Figure 4C, QDs are uniformly distributed in QD-silox film (the inset shows magnified TEM image of QD-silox film). Also, 3-D images of visualized elemental distribution information on QD-silox film are obtained from TOF-SIMS analysis (Figure 4D), in which elements of Si (siloxane matrix), Se (QD core), and Zn (QD shell) are evenly distributed in the cube of  $1000\text{ }\mu\text{m}^3$ . The TEM and TOF-SIMS analyses corroborate that QDs are uniformly dispersed in QD-silox film, indicating that aggregation of QDs does not occur during the film fabrication process based on QD-oligosiloxane resin. As a result, the QD-silox film shows spatially uniform PL, both emission peak wavelength and fwhm, as visualized in dispersive-Raman PL spectroscopy in the area of  $100\text{ }\mu\text{m}^2$  (Figure S3). Consequently, uniform encapsulation of QDs by heat-resisting siloxane network confers the QD-silox film with long-term PL QY stability under harsh environment.

In order to see how QD-silox films behave under moist environment, we monitored the PL QY of QD-silox and QD/acrylate films stored in air at  $85\text{ }^\circ\text{C}$  and  $85\%\text{ RH}$  for 40 days (Figure 5A). To our surprise, the PL QY of the QD-silox film is noticeably enhanced (from  $61.8\%$  to  $73.6\%$ ) in the first 2 days and retains its enhanced PL QY of  $73.6\%$  thereafter, whereas QD/acrylate film exhibits substantial decrease in PL QY from  $61.8\%$  down to  $35.1\%$ . It is also worth noting that the decreased PL QY of the QD/acrylate film aged at  $85\text{ }^\circ\text{C}/85\%\text{ RH}$  is still higher than that of the same film aged at  $85\text{ }^\circ\text{C}/5\%\text{ RH}$ .

The enhanced PL QY of QD-silox film in moisture can be corroborated by PL decay dynamics (Figure 5B). We analyzed PL decay dynamics to characterize the optical properties of QD-silox and QD/acrylate films before and after aging (Figure 5B). As we defined earlier, the  $1/e$  lifetime ( $\tau$ ) of the QD-silox film increases from  $35.3$  to  $48.6\text{ ns}$ , while the QD/acrylate film shows a decrease of  $\tau$  to  $16.1\text{ ns}$ , for 40 days of aging. The PL intensity decay curves of QD-silox and QD/acrylate films before aging are fitted with biexponential decay with two recombination components of radiative ( $\tau_1$ :  $34.4\text{ ns}$ ,  $98.4\%$ ) and delayed ( $\tau_2$ :  $192.2\text{ ns}$ ,  $1.3\%$ ) recombination pathways. After aging, the QD-silox film is fitted with single-exponential decay with increased radiative recombination lifetime ( $\tau_1$ :  $43.2\text{ ns}$ ),

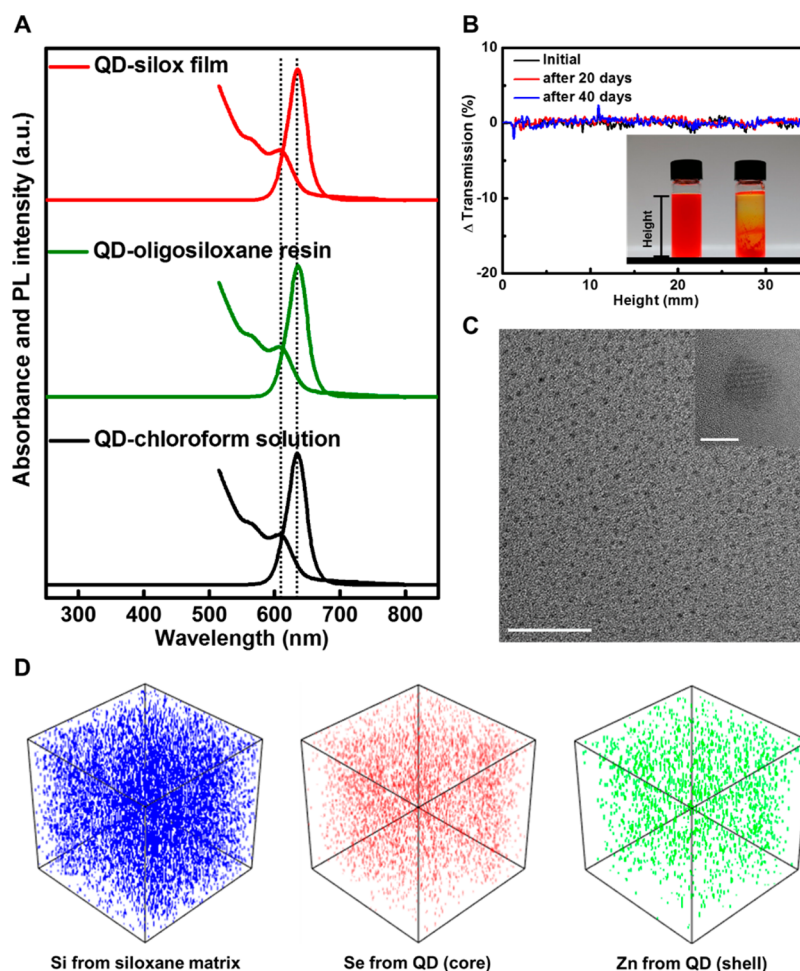


**Figure 4.** (A) Absorbance and PL spectra of QD-chloroform solution (black), QD-oligosiloxane resin (green), and QD-silox film (red). (B) Delta transmission spectra of QD-oligosiloxane resin for 40 days of storage under ambient condition. Inset shows photograph of QD-oligosiloxane resin (left vial) and QD/acrylate resin (right vial) after being stored for 1 h under ambient condition. (C) TEM image of QD-silox film, which film was prepared by FIB instrument (scale bar =50 nm). Inset shows magnified TEM image of QD-silox film (scale bar =5 nm). (D) TOF-SIMS 3-D images of QD-silox film; Si (blue), Se (red), and Zn (green) ( $1000 \mu\text{m}^3$  of cube).

while the curve for the aged QD/acrylate film is fitted on a biexponential model with new fast, nonradiative ( $\tau_1$ : 10.9 ns, 60.2%) and slow, decreased radiative ( $\tau_1$ : 32.0 ns, 39.7%) recombination channels.

Enhanced PL QY of CdSe/ZnS QDs under moist environment has been reported in previous studies in which water molecules are speculated to passivate trap states of QDs.<sup>34,35</sup> Again, evolution of the fast nonradiative decay component observed in this study results in reduced population of radiative recombination pathways, ultimately leading to decreased PL QY of QD/acrylate film in air at 85 °C and 85% RH. From this perspective, both increased radiative (from 34.4 to 43.2 ns) and disappeared delayed recombination pathways of the QD-silox film indicate reduction of trap states after aging which coincide with its enhanced PL QY. In addition, the QD/acrylate film aged at 85 °C/85% RH shows both longer nonradiative and radiative recombination PL lifetime than the same film aged at 85 °C/5% RH. The only difference between 85 °C/5% RH and 85 °C/85% RH environments is the level of moisture. Therefore, we surmise that water molecules passivate trap states of both types of films.<sup>34,35</sup> We conducted further investigation in search for the molecular rationale behind the enhanced PL QY of QD-silox film by water molecules.

Figure 6A shows FT-IR spectra of QD-silox film, before and after storage under a 85 °C/85% RH environment. The bands corresponding to —OH stretching vibrations in the range of  $3700\text{--}3150 \text{ cm}^{-1}$  appear in the case of the aged QD-silox film, hinting at the existence of adsorbed water molecules. Also, Figure 6B shows traces of PL QY of QD-silox film by repetitive aging under water molecule adsorption (85 °C/85% RH) and desorption (85 °C/5% RH) environments. On the basis of Figure 6B, the PL QY of the QD-silox film falls back down to its initial value by desorption of water molecules under aging in dry air at 85 °C and reversibly goes back up after the humidity treatment (i.e., aging at 85 °C/85% RH). This serves as the smoking gun that the adsorbed water molecules result in increased PL QY of the QD-silox film. Therefore, the enhanced PL QY of the QD-silox film after 85 °C/85% RH aging is explained by passivating trap states with the help of adsorbed water molecules.<sup>34,35</sup>

There are two competing reaction mechanisms in the presence of both oxygen and water molecules. At low RH, oxygen is the major oxidation agent which is electron acceptor that promote electron transfer from the QDs.<sup>34,35</sup> Oxygen radical anions result in formation of nonradiative recombination trap states.<sup>35</sup> Conversely, at high RH, water molecules that adsorb on the surface of the QDs appear to minimize the

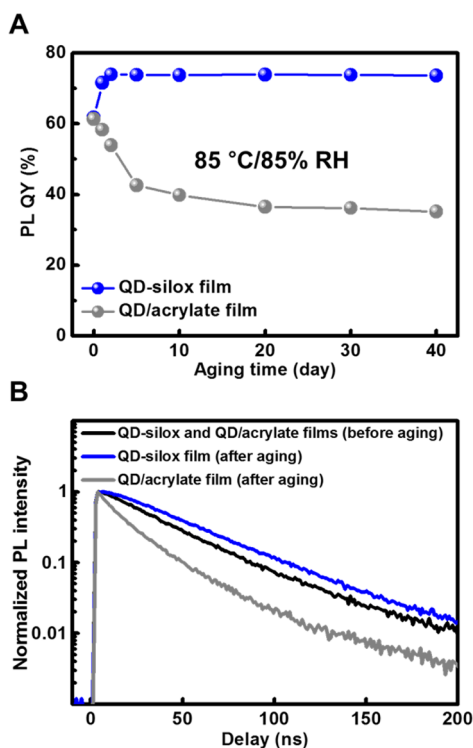


**Figure 5.** (A) Traces of PL QY of QD-silox film (blue) and QD/acrylate film (gray) monitored over 40 days of aging in air at 85 °C and 85% relative humidity (RH). (B) PL decay dynamics of QD-silox and QD/acrylate before (black) and after (blue: QD-silox; and gray: QD/acrylate) aging for 40 days.

detriment of oxidation by oxygen.<sup>35</sup> Comprehensive mechanism for the passivation of trap states via hydration of QD surface is unavailable, yet fluorescence enhancement upon hydration has been reported in the context of competing oxidation mechanisms by water vs oxygen.<sup>35</sup>

Figure 6C shows traces of PL QY of QD-silox film stored at 85 °C and different RHs. The higher the RH at 85 °C, the higher the PL QY of QD-silox film, with the increase being 5.9%, 10.7%, and 11.8% at 25% RH, 55% RH, and 85% RH, respectively, but PL QY remains nearly the same in a dry condition (at 5% RH). Also, a rate at which PL QY of QD-silox films increases appears to depend on moisture level (25% RH: 1.9%/day, 55% RH: 3.5%/day, and 85% RH: 3.9%/day). This result alludes to likelihood that the number of passivated trap states has to do with the amount of adsorbed water molecules in QD-silox film. In addition, we examine the PL QY of the QD-silox and QD/acrylate films over 40 days of aging in strong acidic (0.5 N of hydrochloric acid) and strong basic (0.5 N of sodium hydroxide) solutions under ambient conditions (Figure S4). Coupled with encapsulated QDs by siloxane matrix and adsorbed water molecules in acidic or basic solution, QD-silox film exhibits both enhanced PL QY and long-term stability of PL QY, whereas the PL QY of QD/acrylate film decreases significantly. In addition, when immersed in boiling water (100 °C), the QD-silox film becomes even brighter and its PL QY remains at the increased value at least for 24 h (Figure S5 and Video S1).

## CONCLUSIONS

We prepared siloxane-encapsulated QD film (QD-silox film) by free radical addition reaction using QD-oligosiloxane resin,

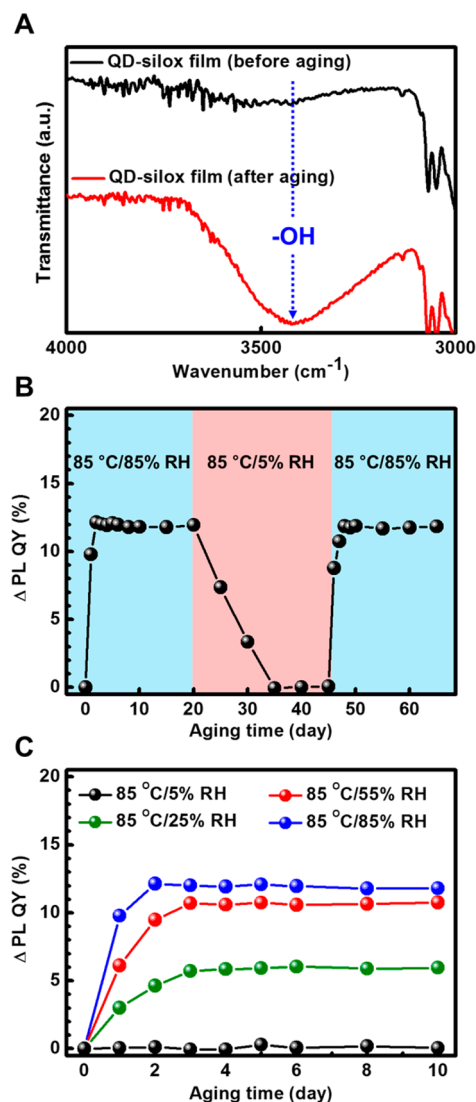


**Figure 6.** (A) FT-IR spectra of QD-silox film before (black) and after (red) aging in air at 85 °C and 85% relative humidity (RH). (B) Trace of PL QY increase of QD-silox film by alternating exposure to 85% RH and 5% RH in air at 85 °C. (C) Traces of PL QY of QD-silox film stored in air at 85 °C and different relative humidity: 5% RH (black); 25% RH (green); 55% RH (red); and 85% RH (blue).

which had been synthesized via sol-gel condensation reaction between silane precursors in the presence of QDs. The synthesized QD-oligosiloxane resin exhibit even dispersion of QDs in the resin and long-term dispersion stability for 40 days under ambient conditions. This dispersion stability of the QD-oligosiloxane resin is attributed to hydrophobic interaction between oleic acid, which is the surface ligand on QDs, and functional groups (methacryl and phenyl) of the oligosiloxane matrix without ligand exchange of QDs. In addition, the free radical addition reaction between oleic acid and the methacryl group improves the thermal stability of the QD-silox film due to formation of additional cross-linking. Consequently, the PL QY of the QD-silox film remains nearly unchanged under various harsh external conditions: 85 °C/5% RH; 85 °C/85% RH; strong acidic; strong basic; and even in boiling water.

The dramatic enhancement in the stability of the composite film under severe conditions, e.g., heat, moisture, acid, and base, resonates profoundly, as the excellent dispersion of QDs in film

and stable optical properties are, in fact, the two key requirements in the down-conversion film in display applications. In particular, noticeably enhanced PL QY of QD-silox film ( $\Delta$ PL QY: + 11.8%) in the presence of water molecules is unprecedented. We observed reversible curing of emission intensity; namely, the enhanced PL QY of QD-silox film is retrieved to its initial value by desorption of water molecules (aging under 85 °C/5% RH) and enhanced again by adsorption of water molecules (aging under 85 °C/85% RH) by passivating trap states. We envision that our siloxane-based passivation will push the envelope of QD composite films as an organic/inorganic hybrid system.

## EXPERIMENTAL SECTION

**Chemicals.** 3-Methacryloxypropyltrimethoxysilane (MPTS) (ShinEtsu, Japan), diphenylsilanediol (DPSD) (Gelest, U.S.A.), barium hydroxide monohydrate, 2,2-dimethoxy-2-phenylacetophenone, octadecylchlorosilane (OTS) (Sigma-Aldrich, U.S.A.), QD (CdSe/ZnS) (Nanodot-HE-series) (Ecoflux, Korea) and diacrylate functionalized aliphatic oligomer resin (Miramer M244) (Miwon Specialty Chemical Co., Ltd., Korea) were purchased and used as received.

**Synthesis of QD-Oligosiloxane Resin.** QD-oligosiloxane resin was synthesized via sol-gel condensation reaction between MPTS (1 mol) and DPSD (1.5 mol) in the presence of QDs (0.5 wt %). MPTS, DPSD, and QDs were blended in a two-neck flask by magnetic stirrer for a few minutes. After the blending, barium hydroxide monohydrate was added as a catalyst to promote sol-gel condensation reaction under 80 °C with N<sub>2</sub> gas purging for a few hours. After the sol-gel condensation reaction, 0.2 wt % of 2,2-dimethoxy-2-phenylacetophenone was added to the QD-oligosiloxane resin for UV-induced free radical addition reaction to fabricated solid-state film.

**Preparation of QD/Acrylate Resin.** QD/acrylate resin prepared by simple blending diacrylate functionalized aliphatic oligomer resin and QDs (0.5 wt %) under 80 °C with N<sub>2</sub> gas purging for a few hours to remove solvent. After the removing solvent, 0.2 wt % of 2,2-dimethoxy-2-phenylacetophenone was added to the QD/acrylate oligomer resin for UV-induced free radical addition reaction to fabricated solid-state film.

**Preparation of QD-Silox and QD/Acrylate Films.** The QD-oligosiloxane and QD/acrylate resins were molded separately in stainless steel frame (1 mm of thickness, 20 mm of radius) covered both sides by glass plates. Glass plates were surface-treated by OTS to facilitate separation of films from glass plates after UV ( $\lambda = 365$  nm)-induced free radical addition reaction.

**Aging Condition of QD-Silox and QD/Acrylate Films.** QD-silox and QD/acrylate films were aged under 85 °C/5% relative humidity (RH); 85 °C/85% RH; 0.5 N of hydrochloric acid; 0.5 N of sodium hydroxide; and in boiling water without exposing films to light (dark condition).

**Characterization.** PL QY values were collected by an absolute PL quantum yield spectrometer, Quantaury-QY C11347 series (Hamamatsu Photovics K.K., Japan) using a Xenon light source (150 W). PL decay curves were obtained from a fluorescence lifetime spectrometer, FL920 (Edinburgh Instruments, England) using 470 nm laser as an excitation source. <sup>29</sup>Si NMR spectrum was obtained from a DMX600 FT 600 MHz (Bruker Biospin, Australia). The FT-IR spectra were recorded with an FT-IR 680 plus (JASCO, U.S.A.). TGA profiles were collected using a TGA Q50 (TA Instruments, U.S.A.) with a ramp of 10 °C min<sup>-1</sup> under N<sub>2</sub>. Absorbance spectra were obtained from a UV-vis-NIR spectrometer, SolidSpec-3700 (Shimadzu, Japan). PL spectra were recorded by a DARS PRO 5100 PL system (PSI Trading Co., Ltd., Korea) using a Xenon light source (500 W) as an incident beam. Delta transmission spectra were measured by the Turbiscan (Formulation, France) using monochromatic light ( $\lambda = 880$  nm). 3-D images of TOF-SIMS were collected by a TOF-SIMSS (ION-TOF GmbH, Germany). 2-D images of dispersive-Raman PL spectrometer were obtained from an ARAMIS (Horiba Jobin Yvon, France). The TEM sample was prepared by a FIB, Nova-200 (FEI

company, Netherlands). TEM image was collected by a JEM-ARM200F (JEOL, Japan).

## ASSOCIATED CONTENT

### Supporting Information

The Supporting Information is available free of charge on the ACS Publications website at DOI: 10.1021/jacs.6b10681.

PL QY of the QD-oligosiloxane resin and QD-silox film prepared with different QD concentrations; TGA profiles of QD-silox film and QD/acrylate film; 2-D images of emission wavelength and fwhm of QD-silox film in the area of 100  $\mu$ m<sup>2</sup>; traces of PL QY of QD-silox film and QD/acrylate film monitored over 40 days of aging in acidic (0.5 N of hydrochloric acid) and basic (0.5 N of sodium hydroxide) solutions under ambient conditions; trace of PL QY of QD-silox film monitored over 24 h of aging in boiling deionized water, photograph of QD-silox films in boiling deionized water under UV lamp ( $\lambda = 365$  nm); PL QY of diluted samples of QD-chloroform solution and QD-oligosiloxane resin; chemical shift and peak area of Si atoms with different bond states in QD-oligosiloxane resin and formula for DOC calculation; 1S peak wavelength, emission peak wavelength and fwhm of QD-chloroform solution, QD-oligosiloxane resin, and QD-silox film (PDF)

Video of QD-silox films in boiling deionized water (AVI)

## AUTHOR INFORMATION

### Corresponding Authors

\*dclee@kaist.edu

\*bsbae@kaist.ac.kr

### ORCID

Hwea Yoon Kim: 0000-0002-1451-7591

Joon Ha Chang: 0000-0001-8877-9917

Doh C. Lee: 0000-0002-3489-6189

Byeong-Soo Bae: 0000-0001-9424-1830

### Notes

The authors declare no competing financial interest.

## ACKNOWLEDGMENTS

This work was supported by the Wearable Platform Materials Technology Center (WMC) funded by the National Research Foundation of Korea (NRF) Grant of the Korean Government (MSIP) (NRF-2016R1A5A1009926 and NRF-2016M3A7B4910618). This research was also supported by a grant from the Korea Evaluation Institute of Industrial Technology (Project 10051337).

## REFERENCES

- (1) Murray, C.; Norris, D. J.; Bawendi, M. G. *J. Am. Chem. Soc.* **1993**, *115*, 8706–8715.
- (2) Norris, D.; Bawendi, M. *Phys. Rev. B: Condens. Matter Mater. Phys.* **1996**, *53*, 16338.
- (3) Peterson, M. D.; Cass, L. C.; Harris, R. D.; Edme, K.; Sung, K.; Weiss, E. A. *Annu. Rev. Phys. Chem.* **2014**, *65*, 317–339.
- (4) Hines, D. A.; Kamat, P. V. *ACS Appl. Mater. Interfaces* **2014**, *6*, 3041–3057.
- (5) Woo, J. Y.; Ko, J.-H.; Song, J. H.; Kim, K.; Choi, H.; Kim, Y.-H.; Lee, D. C.; Jeong, S. *J. Am. Chem. Soc.* **2014**, *136*, 8883–8886.
- (6) Woo, J. Y.; Lee, S.; Lee, S.; Kim, W. D.; Lee, K.; Kim, K.; An, H. J.; Lee, D. C.; Jeong, S. *J. Am. Chem. Soc.* **2016**, *138*, 876–883.
- (7) Lee, J.; Sundar, V. C.; Heine, J. R.; Bawendi, M. G.; Jensen, K. F. *Adv. Mater.* **2000**, *12*, 1102–1105.

- (8) Kim, K.; Woo, J. Y.; Jeong, S.; Han, C. S. *Adv. Mater.* **2011**, *23*, 911–914.
- (9) Cho, S.; Kwag, J.; Jeong, S.; Baek, Y.; Kim, S. *Chem. Mater.* **2013**, *25*, 1071–1077.
- (10) Fogg, D.; Radzilowski, L.; Dabbousi, B.; Schrock, R.; Thomas, E.; Bawendi, M. *Macromolecules* **1997**, *30*, 8433–8439.
- (11) Skaff, H.; Sill, K.; Emrick, T. *J. Am. Chem. Soc.* **2004**, *126*, 11322–11325.
- (12) Odoi, M. Y.; Hammer, N. I.; Sill, K.; Emrick, T.; Barnes, M. D. *J. Am. Chem. Soc.* **2006**, *128*, 3506–3507.
- (13) Jeong, S.; Achermann, M.; Nanda, J.; Ivanov, S.; Klimov, V. I.; Hollingsworth, J. A. *J. Am. Chem. Soc.* **2005**, *127*, 10126–10127.
- (14) Kim, S.; Bawendi, M. G. *J. Am. Chem. Soc.* **2003**, *125*, 14652–14653.
- (15) Bullen, C.; Mulvaney, P. *Langmuir* **2006**, *22*, 3007–3013.
- (16) Dubois, F.; Mahler, B.; Dubertret, B.; Doris, E.; Mioskowski, C. *J. Am. Chem. Soc.* **2007**, *129*, 482–483.
- (17) Wang, X.-S.; Dykstra, T. E.; Salvador, M. R.; Manners, I.; Scholes, G. D.; Winnik, M. A. *J. Am. Chem. Soc.* **2004**, *126*, 7784–7785.
- (18) Pong, B.-K.; Trout, B. L.; Lee, J.-Y. *Langmuir* **2008**, *24*, 5270–5276.
- (19) Dabbousi, B. O.; Rodriguez-Viejo, J.; Mikulec, F. V.; Heine, J. R.; Mattoussi, H.; Ober, R.; Jensen, K. F.; Bawendi, M. G. *J. Phys. Chem. B* **1997**, *101*, 9463–9475.
- (20) Mancini, M. C.; Kairdolf, B. A.; Smith, A. M.; Nie, S. *J. Am. Chem. Soc.* **2008**, *130*, 10836–10837.
- (21) Chen, J.; Hardev, V.; Yurek, J. *Inf. Display.* **2013**, *29*, 12–17.
- (22) Reetz, M. T. *Adv. Mater.* **1997**, *9*, 943–954.
- (23) Gill, I.; Ballesteros, A. *J. Am. Chem. Soc.* **1998**, *120*, 8587–8598.
- (24) Kwak, S. Y.; Yang, S.; Kim, N. R.; Kim, J. H.; Bae, B. S. *Adv. Mater.* **2011**, *23*, 5767–5772.
- (25) Wu, J.; Mather, P. T. *Polym. Rev.* **2009**, *49*, 25–63.
- (26) Rabouw, F. T.; Kamp, M.; van Dijk-Moes, R. J.; Gamelin, D. R.; Koenderink, A. F.; Meijerink, A.; Vanmaekelbergh, D. *Nano Lett.* **2015**, *15*, 7718–7725.
- (27) Gao, X.; Cui, Y.; Levenson, R. M.; Chung, L. W.; Nie, S. *Nat. Biotechnol.* **2004**, *22*, 969–976.
- (28) Rizvi, S. B.; Yang, S. Y.; Green, M.; Keshtgar, M.; Seifalian, A. M. *Bioconjugate Chem.* **2015**, *26*, 2384–2396.
- (29) Kim, S. Y.; Augustine, S.; Eo, Y. J.; Bae, B. S.; Woo, S. I.; Kang, J. K. *J. Phys. Chem. B* **2005**, *109*, 9397–9403.
- (30) Jin, J.; Yang, S.; Bae, B.-S. *J. Sol-Gel Sci. Technol.* **2012**, *61*, 321–327.
- (31) Tsavalas, J. G.; Luo, Y.; Schork, F. J. *J. Appl. Polym. Sci.* **2003**, *87*, 1825–1836.
- (32) Okamoto, M.; Morita, S.; Taguchi, H.; Kim, Y. H.; Kotaka, T.; Tateyama, H. *Polymer* **2000**, *41*, 3887–3890.
- (33) Jun, S.; Lee, J.; Jang, E. *ACS Nano* **2013**, *7*, 1472–1477.
- (34) Müller, J.; Lupton, J.; Rogach, A.; Feldmann, J.; Talapin, D.; Weller, H. *Appl. Phys. Lett.* **2004**, *85*, 381–383.
- (35) Pechstedt, K.; Whittle, T.; Baumberg, J.; Melvin, T. *J. Phys. Chem. C* **2010**, *114*, 12069–12077.